

BIOSIGNATURE SCREENING IN MODERN WET AEOLIAN ENVIRONMENTS USING X-RAY FLUORESCENCE AND X-RAY DIFFRACTION TECHNOLOGIES. H.J. Patel¹, R.C. Ewing¹, M.M. Tice¹, M. Nachon¹, Texas A&M University, Department of Geology and Geophysics, 3115 TAMU, College Station, TX 77843, harsh.patel_1993@tamu.edu

Introduction: Wet aeolian environments on Earth host microbial life [1, 2]. Similar environments have been identified in the stratigraphy of Mars [3], and are potential targets for the exploration of ancient Martian life. Despite the recognition that wet aeolian systems contain life and were present on ancient Mars, little is known about potential textural and geochemical biosignatures in these deposits.

To explore for possible biosignatures in wet aeolian environments, our study examined textural and geochemical characteristics of microbially-influenced wet aeolian deposits at Padre Island, Texas. Work was conducted at Padre Island National Seashore (PAIS), Texas. PAIS is a 104 km long barrier island along the southern Texas Gulf of Mexico (GOM) coastline. We examined microbially colonized interdunes and sabkha deposits on the back-barrier part of the island.

Methods: Our methods include trenching, measured sections, *in-situ* handheld x-ray fluorescence (XRF) analysis, laboratory micro XRF analysis, and laboratory x-ray diffraction (XRD) analysis to study the deposits.

1) *Trenching* - We dug trenches ~50 cm deep near dune fields to characterize microbial mat-influenced interdune stratigraphy. Epoxy adhesive sediment peels from trench walls were collected for laboratory XRF and XRD analysis (Fig. 1A).

2) *XRF analyses* - A portable handheld XRF was used to characterize the *in-situ* geochemistry of the surface crusts and trench stratigraphy. This tool is useful to detect microbial alteration of redox-active heavy mineral deposits (established through laboratory XRD analysis). Sediment peels were mapped using a Horiba XGT-7000 micro XRF to create a two-dimensional (2-D) elemental map of the trench walls (Fig. 1B). 2-D elemental maps were used to characterize textural distinction between microbially influenced and aeolian strata.

3) *XRD analysis* - Loose samples from crusted (biotic) and non-crusted (abiotic) strata from the PAIS were analyzed in the laboratory XRD to assess redox-sensitive mineralogy and examine their alteration before (surficial deposits) and after burial.

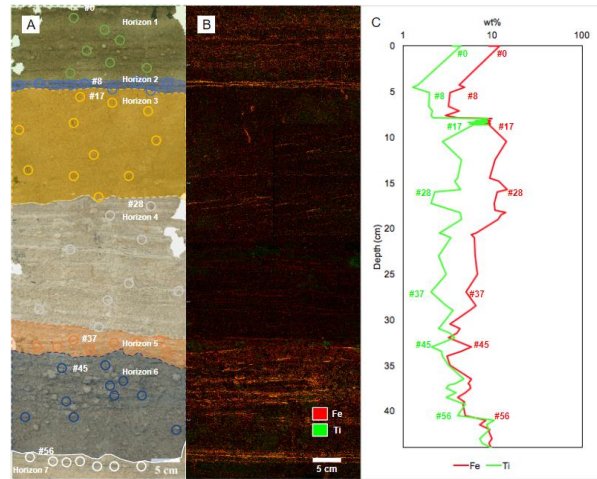


Figure 1: *In-situ* handheld and laboratory micro XRF analysis. (A) Sediment peel with marked handheld XRF analysis locations and horizons for a trench dug in PAIS in Aug. 2018. (B) 100 μ m two-dimensional elemental map of sediment peel in (A). Fe and Ti appear red and green in the element map and correlate to dark laminations in (A). (C) Elemental profile of Fe and Ti at marked locations in (A).

Results: We grouped and separated identical strata in the sediment peels into eight horizons (Fig. 1A). Horizon 0 (not illustrated in the figure) is the crinkly/wavy, ~1cm thick surface microbial mat crust. Texture for this stratum is a result of bacteria bounding surface grains. Horizon 1 is classified as crude, brown lamination with a spongy texture. Individual laminations in this stratum are ~1 to 2mm thick and have a wavy, continuous pattern. The sponge texture arises from air bubbles displacing grains; a by-product of organic matter decay in the stratum. Horizon 2 and 7 are dark, aeolian lag deposits, primarily composed of heavy minerals. Horizon 3 is classified as cross-stratification. The sets are ~1cm and ~5cm thick, respectively. Preferential deposition of heavy minerals occurs at bounding surfaces. Horizons 2, 3, and 7 appear dominated by wind transport. Grey laminated horizons 4 and 5 are sand and clay layer deposits hypothesized to be linked to vegetation growth. Horizon 6 is thin (~1 to 2mm), black, semi-continuous laminations. Based on texture similarity to the ones observed on the surface, we think these laminations are adhesion ripples with microbial influence.

In-situ handheld and laboratory micro XRF analyses of sediment peels and loose sediment samples from two trenches indicate that strata associated with microbial mats (Horizons 1 and 6) have distinct Fe, Ti, and Zr (not shown) signatures compared to strata that is not clearly microbially influenced (Fig. 1B and 1C). Preliminary results from Fe/Ti and Ti/Si wt% ratio relationship indicate that Ti/Si ratio of the inferred buried microbial material in Horizon 1 and in Horizon 6 remains similar to that of the surface microbial crusts, aeolian lag deposits (Horizon 2 and 7), and trough cross-beds (Horizon 3), however, the Fe/Ti ratio decreases. This shift in the Fe/Ti ratio is interpreted as the reduction of Fe during decay of buried mats.

XRD mineralogical assessment of loose sediment samples identified ilmenite (FeTiO_3), rutile (TiO_2), goethite (Fe(III)OH), and magnetite (Fe_3O_4). The abundances of these minerals vary by horizon in the trenches. Microbially influenced horizons have significantly lower ilmenite abundances than abiotic deposits (Fig. 3; $p=0.003$, single-factor ANOVA). This relationship is consistent for samples from both trenches. Because ilmenite and rutile grains have similar sizes and densities, lower ilmenite: rutile ratios in buried mats likely do not form by differential transportation or deposition. Instead, we hypothesize that ilmenite is oxidized in actively photosynthesizing mats, redepositing Fe as ferric oxyhydroxides or goethite. During mat burial and degradation, this Fe is reduced and leached from the sediment profile, resulting in lower Fe/Ti and ilmenite: rutile ratios.

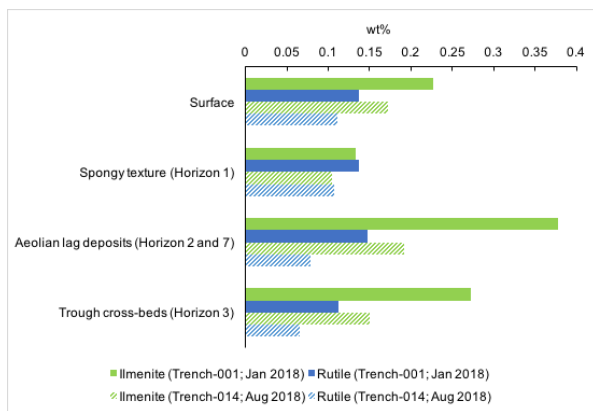


Figure 3: Laboratory XRD analysis of loose sediment samples from PAIS. Ilmenite (FeTiO_3) wt% composition is significantly lower in spongy buried crust. Rutile (TiO_2) wt% composition is relatively consistent across all samples.

References:

- [1] Crabaugh, M. et al. (1993), *Geol. Soc. Spec. Publ.*, 72.1, 103-126. [2] Knoll, A.H. (1985), *Hypersaline Ecosystems*, Springer-Verlag, 53. [3] Grotzinger, J. P. et al. (2005), *Earth Planet Sc. Lett.*, 240.1, 11-72. [4] Al-Masrahy, M.A. et al. (2015), *Aeolian Res.*, 17, 67-88.